Optical model of clouds as derived from airborne measurements of shortwave solar radiation

I.N. Melnikova

Scientific & Research Center for Ecological Safety, Russian Academy of Sciences, St. Petersburg

Received January 24, 2001

Optical spectral parameters of stratus clouds (single scattering albedo and optical thickness, as well as scattering and absorption coefficients) in shortwave spectral region are important as input parameters for many problems of atmospheric optics and climate. Here we analyze the results obtained from airborne, ground-based, and space measurements at different geographical sites for more than 30 years. Optical parameters were reconstructed from observations of hemispherical fluxes and intensity of solar radiation using analytical solution of the inverse problem. Spectral dependence, vertical profiles, and geographic distribution of optical parameters of stratus clouds are presented. Three main types of the clouds with weak, intermediate, and strong light absorption are revealed. Noticeable dependence of the volume scattering coefficient on the radiation wavelength is found.

Introduction

Optical models of clouds are needed for radiative calculations of the cloudy atmosphere, simulation of extended cloudiness in problems of weather forecast, and study of global climate changes.[1–4] The importance of developing adequate optical models for proper consideration of stratus in climatic calculations is beyond doubt, therefore development of an optical model of clouds is an urgent problem. The values of stratus optical parameters can be applied both to calculation of shortwave radiation budget of the atmosphere and its components under stratus conditions and to research into stratus clouds themselves.

The optical parameters have been obtained from ten airborne and three ground-based experiments including measurements of shortwave radiation in the wavelength region of 0.35–0.95 μm in the cloudy atmosphere, as well as from satellite measurements by POLDER and AVHRR devices. Airborne observations have been conducted for more than 30 years in different geographic zones.[5–11] Space observations also cover extended areas.[13,14] Thorough description of the measurement technique and tentative processing of the data can be found in Refs. 5–7, 10, 15, and 17. The method of reconstruction of optical parameters and results of processing of particular experiments are described in Refs. 13, 14, and 19–30. The single scattering albedo ω_0 and the optical thickness τ (or volume coefficients of scattering α and absorption k) were determined independently for every wavelength from the data of spectral measurements. This paper gives spectral values of the optical thickness τ and single scattering albedo ω_0, as well as the volume scattering α and absorption k coefficients smoothed and averaged over different realizations. These values include the absorption by gases in the shortwave region and can be used as input parameters in radiative calculations for the cloudy atmosphere. The effect of reflection from the underlying surface was taken into account when processing all the considered measurements.

Main details of reconstruction of optical parameters from radiative measurements are presented. Spectral dependence of the optical thickness and the volume scattering coefficient, as well as single scattering albedo and the volume absorption coefficient obtained from processing of radiative measurements is analyzed. Disagreement between the obtained values and the values calculated by the Mie theory is explained. The vertical behavior of scattering and absorption coefficients is further discussed. In closing some conclusions and recommendations are given.

Radiative spectral measurements

Optical properties of some cloud layer are characterized by the optical thickness τ and the single scattering albedo ω_0, as well as the volume scattering α and absorption k coefficients. These parameters were obtained from airborne and ground-based spectral measurements of shortwave solar radiation.[5–12] The spectrometer used in the experiments was designed and calibrated specially for measurements of solar radiation in the atmosphere.[15] The device, used in the experiment,[11] is described in Ref. 16.

It should be emphasized that for obtaining optical parameters from airborne measurements we chose such radiative experiments, which were conducted in optically thick and horizontally homogeneous extended stratus clouds. All measurements were conducted over some vast homogeneous underlying surface (water surface, snowed surface, desert, etc.). Under these conditions, factors hampering our analysis, such as horizontal inhomogeneity of clouds, inhomogeneity of the surface, broken clouds, sink of radiation through side boundaries of a cloud, and inhomogeneous

0235-6880/01/08 651-11 $02.00

meteorological conditions can be ignored. The errors of radiative measurements varied within 1–5%. Table 1 lists all used experiments and presents some additional information on their conditions. It also gives the values of the surface albedo A, optical thickness τ, and single scattering albedo ω_0, as well as the volume scattering α and absorption k coefficients for 0.5 μm wavelength. The experiments 1–7 and 9–11 were conducted aboard the aircraft,[5–9] and experiments 8, 12, and 13 are ground-based.[10,11]

The measurements were conducted within the framework of the CAENEX, GAAREX, POLEX, and GATE experiments and other programs in different latitude zones from 16 to 85°N (Refs. 5–10). The airborne experiments included measurements above, under, and, in some cases, inside clouds. In all cases, spectral absorption of solar radiation inside cloud layers was observed.[5–9] Vertical sensing of stratus was made in airborne experiments over Lake Ladoga (experiments 6 and 7, Refs. 7, 9, 12) and the Kara Sea (experiment 9, Ref. 8).

When averaging optical parameters of stratus, the satellite data (ADEOS-I, NOAA-12, and NOAA-14; Refs. 13 and 14) were also taken into account.

Optical parameters of clouds as derived from solar radiation measurements

The values of the single scattering albedo and optical thickness were obtained from radiative measurements by the method developed and thoroughly described in Refs. 17–23 and 25, where the analysis of errors also is given. Both parameters were determined for each wavelength independently of their values at other wavelengths. The errors of reconstruction of the optical thickness depend on absorption in a cloud layer: as absorption increases, the errors increase too. However, in the shortwave region, absorption of radiation in clouds is rather low even in molecular absorption bands, and this allows τ to be determined quite reliably. The errors of reconstruction of the single scattering albedo ω_0 increase at the low optical thickness. On the average, the single scattering albedo is determined accurate to 3–6%, and the optical thickness is determined with the error of 5–10%. The spectral values of the optical thickness and the single scattering albedo are shown in Figs. 1 and 2; Figure 3 shows the volume scattering and absorption coefficients.

Table 1. Measurements of solar radiation and optical parameters of stratus

#	Experiment	φ, °N	Date	A	τ_0	ω_0	α, km^{-1}	k, km^{-1}	R, W/m^2
	ATEP								
1	The Atlantic Ocean	16	07.12.74	0.08	18	0.995	17	0.15	18.9
2	» »	17	08.04.74	0.06	10	0.993	33	0.30	26.1
	CAENEX								
3	The Black Sea	44	04.10.71	0.06	22	0.999	30	0.05	2.9
4	The Sea of Azov	47	10.05.72	0.06	26	0.996	45	0.12	12.8
5	Rustavi	42	12.05.72	0.18	8.0	0.985	7.0	0.10	15.0
6	Lake Ladoga	60	09.24.72	0.20	75	0.996	20	0.12	3.6
7	» »	60	04.20.85	0.64	12	0.998	25	0.05	4.5
8	Petrodvorets	60	04.12.96	0.70	–	0.998	–	–	–
	POLEX								
9	The Kara Sea	75	10.01.72	0.40	4,5	0.990	9.0	0.15	4.6
10	» »	75	05.29.76	0.40	5,4	0.950	1.8	0.08	7.3
11	» »	75	05.30.76	0.05	8,0	1.0	11.4	0.0	1.1
12	Arctic drifting station	85	08.13.79	0.55	17	0.998	–	0.06	–
13	SP-22	85	10.08.79	0.90	17	0.997	–	0.10	–

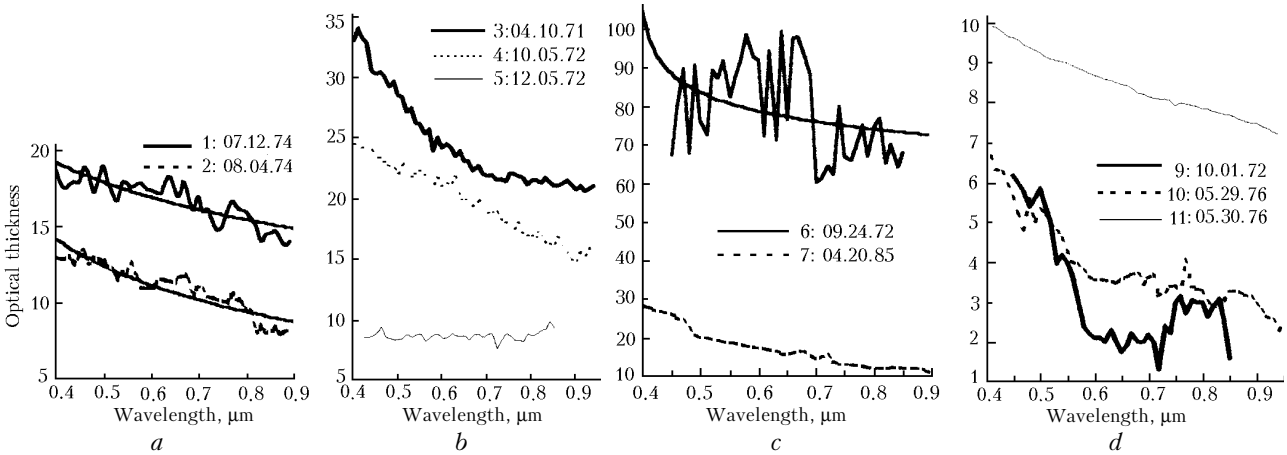

Fig. 1. Spectral dependence of optical thickness τ determined from results of airborne radiative measurements in different latitude zones; the corresponding experiments are numbered as in Table 1.

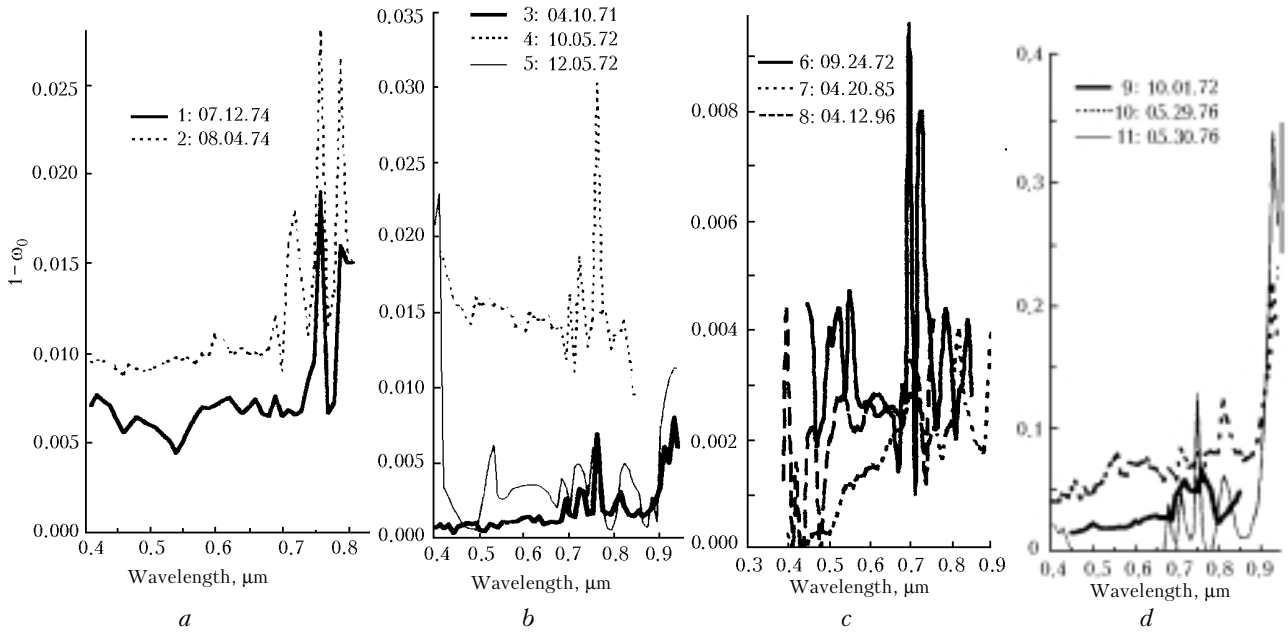

Fig. 2. Spectral dependence of single scattering albedo ω_0 determined from results of airborne radiative measurements in different latitude zones; the corresponding experiments are numbered as in Table 1.

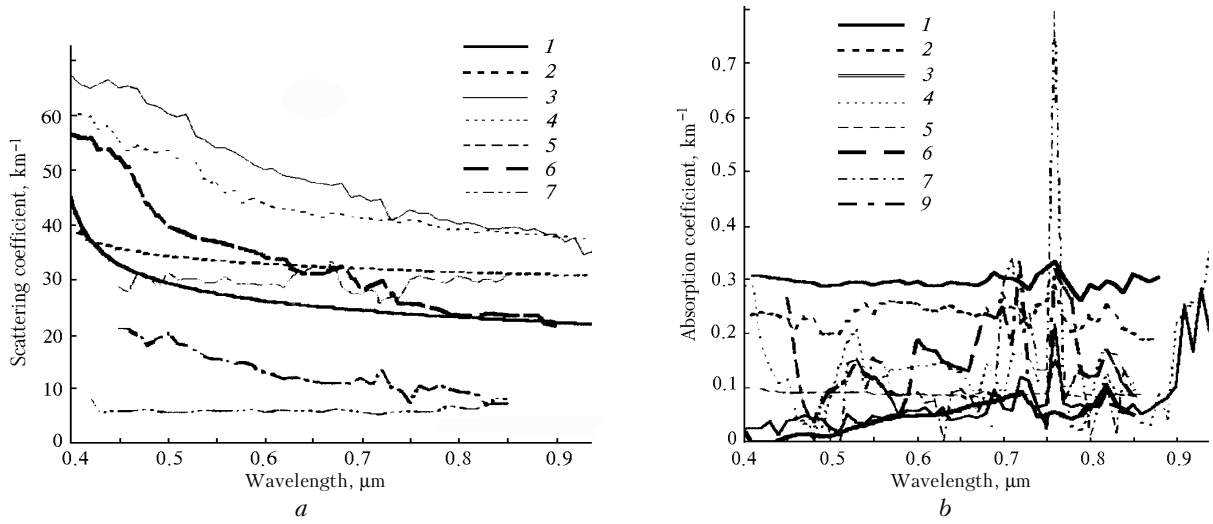

Fig. 3. Volume scattering α (*a*) and absorption *k* (*b*) coefficients of stratus; the corresponding experiments are numbered as in Table 1.

Analysis of these results allows us to divide stratus clouds into three main groups according to the value of the single scattering albedo: clouds with weak absorption (low content of atmospheric aerosol absorbing radiation) above water or snow surface, clouds with medium absorption (continental clouds with medium content of atmospheric aerosol), and clouds with strong absorption (highly polluted clouds containing large amounts of sand or soot aerosols). The smoothed and averaged (over different realizations) spectral values of the optical thickness and single scattering albedo, as well as volume scattering and absorption coefficients for these three types of clouds are given in Table 2. These values include the absorption by gases in the shortwave spectral region and can be used as input parameters in radiative calculations for the cloudy atmosphere.

Optical thickness and volume scattering coefficient

Averaged values of optical thickness τ are given in Table 2, and the scattering coefficient α is shown in Fig. 4*a*. The optical thickness τ within 15–20 proves to be most typical for such clouds. In the experiments under consideration, the optical thickness τ was less than 10 in latitude 75°N and about 20 in the Arctic. The volume scattering coefficient α varied within 20–70 km^{-1}.

Table 2. Optical parameters of stratus

λ,	Clear cloud				Continental cloud				Polluted cloud			
μm	α, km $^{-1}$	k, km $^{-1}$	τ_0	ω_0	α, km $^{-1}$	k, km^{-1}	τ_0	ω_0	α, km $^{-1}$	k, km $^{-1}$	τ_0	ω_0
0.35	64.3	0.0301	32.0	0.99966	32.6	0.1053	16.3	0.99701	8.2	0.3012	11.7	0.96393
0.37	63.4	0.0216	31.7	0.99966	32.2	0.1004	16.2	0.99701	7.9	0.2994	11.5	0.96342
0.39	62.3	0.0168	31.2	0.99966	32.0	0.0992	16.0	0.99701	7.8	0.2933	11.4	0.96232
0.40	61.7	0.0145	30.8	0.99966	31.9	0.0987	15.9	0.99701	7.4	0.3069	11.3	0.96104
0.41	61.1	0.0133	30.6	0.99966	31.7	0.0983	15.8	0.99703	7.2	0.3065	10.0	0.95945
0.42	60.3	0.0129	30.2	0.99966	31.5	0.0961	15.7	0.99705	6.9	0.3055	9.9	0.95833
0.43	59.5	0.0100	29.8	0.99966	31.4	0.0945	15.7	0.99712	6.8	0.3031	9.9	0.95731
0.44	58.5	0.0077	29.2	0.99966	31.3	0.0937	15.6	0.99713	6.7	0.3004	9.8	0.95727
0.45	57.4	0.0228	28.7	0.99966	31.2	0.0927	15.6	0.99711	6.6	0.2954	9.5	0.95697
0.46	56.6	0.026	28.3	0.99955	31.1	0.0922	15.5	0.99709	6.5	0.2966	9.4	0.95642
0.47	55.5	0.0309	27.7	0.99947	30.9	0.0920	15.5	0.99707	6.4	0.2946	9.3	0.95632
0.48	54.5	0.0281	26.5	0.99947	30.7	0.0917	15.5	0.99707	6.4	0.2932	9.3	0.95619
0.49	53.2	0.0277	26.1	0.99947	30.5	0.0915	15.5	0.99707	6.4	0.2895	9.3	0.95615
0.50	51.7	0.0192	25.6	0.99945	30.3	0.0912	15.4	0.99708	6.3	0.2878	9.2	0.95606
0.51	50.5	0.0186	25.1	0.9994	30.1	0.091	15.3	0.99705	6.3	0.2889	9.1	0.95567
0.52	49.2	0.0323	24.6	0.99935	29.8	0.0905	15.1	0.99703	6.3	0.2903	9.1	0.95502
0.53	48.3	0.0352	24.2	0.99934	29.5	0.0903	14.9	0.99702	6.2	0.2938	9.0	0.95492
0.54	47.0	0.0383	23.5	0.99931	29.0	0.0900	14.6	0.99702	6.2	0.2955	9.0	0.95454
0.55	46.3	0.0405	23.1	0.99925	28.6	0.0894	14.2	0.99697	6.2	0.2967	8.9	0.95412
0.56	45.4	0.0416	22.7	0.99908	28.1	0.0883	14.0	0.99695	6.2	0.2974	8.9	0.95387
0.57	44.8	0.0452	22.2	0.99901	27.4	0.0876	13.7	0.99686	6.1	0.2983	8.9	0.95316
0.58	44.2	0.0481	22.1	0.99898	27.0	0.0873	13.5	0.99682	6.1	0.2977	8.9	0.95352
0.59	43.2	0.0520	21.6	0.99877	26.8	0.0868	13.4	0.99674	6.1	0.2962	8.9	0.95376
0.60	42.7	0.0544	21.4	0.99876	26.5	0.0865	13.3	0.99674	6.1	0.2942	8.9	0.95414
0.61	42.0	0.0553	21.0	0.99866	26.4	0.0864	13.4	0.99674	6.1	0.2937	8.8	0.95416
0.62	41.7	0.0571	20.9	0.99864	26.2	0.0864	13.0	0.99672	6.1	0.2925	8.8	0.95404
0.63	41.2	0.0573	20.6	0.99864	25.7	0.0864	12.8	0.99663	6.1	0.2927	8.8	0.95372
0.64	40.6	0.0550	20.3	0.99863	25.4	0.0864	12.7	0.99662	6.1	0.2931	8.8	0.95379
0.65	40.3	0.0517	20.2	0.99857	25.2	0.0864	12.7	0.99661	6.1	0.295	8.8	0.95356
0.66	40.0	0.056	20.0	0.99855	24.9	0.0864	12.7	0.99661	6.0	0.2885	8.8	0.95337
0.67	39.7	0.058	19.8	0.99848	24.6	0.0864	12.7	0.99661	6.0	0.296	8.8	0.95328
0.68	39.4	0.0619	19.7	0.99843	24.0	0.0871	12.7	0.99659	6.0	0.3051	8.7	0.95243
0.69	38.8	0.0856	19.4	0.99785	23.3	0.0945	12.7	0.99648	6.0	0.3172	8.7	0.9508
0.70	38.6	0.0697	19.3	0.99821	22.9	0.0863	11.8	0.99667	6.0	0.2939	8.7	0.95351
0.71	38.2	0.0667	19.2	0.99826	22.6	0.0821	11.7	0.99629	6.0	0.2981	8.7	0.95291
0.72	37.7	0.1042	19.1	0.99727	22.3	0.1099	11.6	0.99613	6.0	0.3100	8.7	0.95130
0.73	37.1	0.0869	18.6	0.99766	21.8	0.0876	11.5	0.99621	6.0	0.3053	8.7	0.95249
0.74	36.6	0.0543	18.1	0.99851	21.2	0.0862	11.5	0.99623	6.0	0.3031	8.7	0.95199
0.75	35.9	0.0527	17.8	0.99852	20.7	0.0876	11.5	0.99624	6.0	0.3282	8.7	0.94742
0.76	35.6	0.1366	17.7	0.99616	20.3	0.1523	11.4	0.99453	6.0	0.3480	8.7	0.94707
0.77	35.3	0.0737	17.6	0.99791	19.9	0.0869	11.3	0.99635	6.0	0.3245	8.7	0.94869
0.78	34.9	0.0517	17.4	0.99852	19.7	0.0848	11.2	0.99609	6.0	0.2933	8.7	0.95249
0.79	34.5	0.0526	17.2	0.99848	19.5	0.0864	11.1	0.99619	6.0	0.2900	8.7	0.95375
0.80	34.2	0.0613	17.1	0.99821	19.3	0.0864	10.6	0.99571	6.0	0.2927	8.7	0.95319
0.81	34.1	0.0714	17.1	0.99791	19.2	0.0848	9.7	0.99569	6.0	0.2959	8.7	0.95301
0.82	33.9	0.0961	16.9	0.99717	19.1	0.1102	9.6	0.99564	6.0	0.2986	8.7	0.95281
0.83	33.6	0.0804	16.8	0.99761	19.1	0.0862	9.5	0.99559	6.0	0.2947	8.7	0.95224
0.84	33.4	0.0551	16.7	0.99825	19.0	0.0864	9.5	0.99553	6.0	0.3094	8.7	0.95096
0.85	33.2	0.0512	16.7	0.99835	19.0	0.0864	9.5	0.99532	6.0	0.3004	8.7	0.95232
0.86	33.0	0.0453	16.6	0.99846	19.0	0.0864	9.5	0.99502	6.0	0.3011	8.7	0.95223
0.87	32.7	0.0551	16.6	0.99846	19.0	0.0864	9.5	0.99434	6.0	0.3027	8.7	0.95197
0.88	32.4	0.0582	13.6	0.99833	19.0	0.0864	9.5	0.99387	6.0	0.3023	8.7	0.95124
0.89	32.1	0.0721	16.4	0.99781	19.0	0.1235	9.5	0.99321	6.0	0.3148	8.7	0.95015
0.90	31.7	0.0926	16.2	0.99715	19.0	0.1371	9.5	0.99182	6.0	0.3399	8.7	0.94639
0.91	31.9	0.1698	16.0	0.99571	19.0	0.1679	9.5	0.98684	6.0	0.3497	8.7	0.94493
0.92	31.3	0.1730	15.7	0.99503	19.0	0.2533	9.5	0.99037	6.0	0.3315	8.7	0.94764
0.93	30.9	0.1827	15.5	0.99412	19.0	0.2456	9.5	0.98724	6.0	0.3413	8.7	0.94617
0.94	30.8	0.1533	15.5	0.99512	19.0	0.2366	9.5	0.98803	6.0	0.3441	8.7	0.94589
0.95	30.7	0.1476	15.4	0.99522	19.0	0.2240	9.5	0.98828	6.0	0.3462	8.7	0.94545

Ground-based measurements failed to determine this coefficient, because the geometric thickness of clouds was unknown. In all cases, the optical thickness has a pronounced spectral dependence (see Fig. 2). This result was confirmed by the data obtained by Asano,[24] namely, the optical thickness in the near-infrared spectral region proved to be half as large as that in the shortwave region. Below we give our explanation to this result. In the region $0.8 < \lambda < 0.95$ μm, the value of α varies within 6–34 km^{-1}.

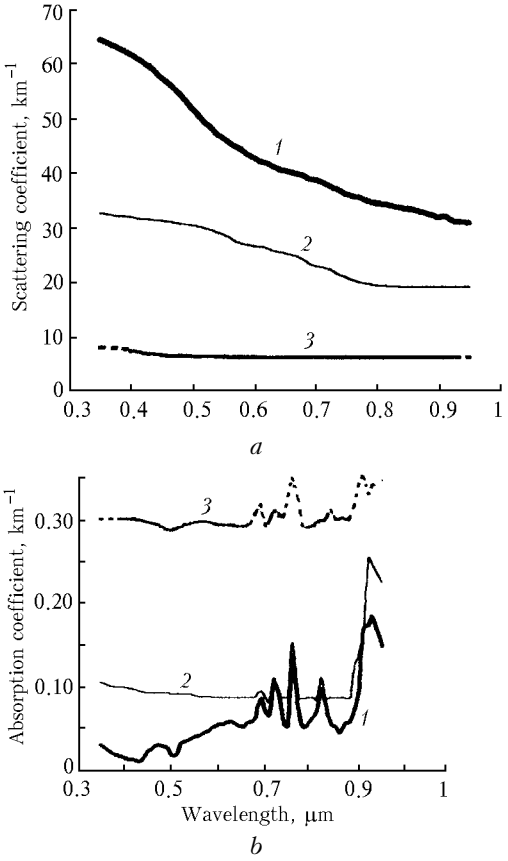

Fig. 4. Volume scattering α (*a*) and absorption k (*b*) coefficients for three models of stratus cloud: clear cloud (*1*), continental cloud (*2*), and polluted cloud (*3*).

Single scattering albedo and volume absorption coefficient

Smoothed values of the single scattering albedo ω_0 are given in Table 2, and the absorption coefficient k is shown in Fig. 4*b*. In the obtained results, the absorptions by aerosol and gas are not separated. As was mentioned above, clouds can be divided into three types based on the results obtained beyond gas absorption bands. *The first type* is characterized by $\omega_0 \sim 0.9997$ and is connected with weak absorption (see Table 2, clear cloud). The corresponding results were obtained in the polar regions and over Lake Ladoga. It follows from the processing of satellite measurements that such values are also characteristic of clouds over oceans. *The second type* of clouds is characterized by intermediate values $\omega_0 \sim 0.9970$–0.9900 and is observed over continents. *The third type* of clouds has very low values of ω_0 from 0.9900 to 0.9500, which are indicative of significant absorption of radiation due to high content of sand or soot in a cloud (for example, the results obtained from experiments 1, 2, and 5).

The absorption coefficient varies from less than 0.05 km^{-1} in clear clouds (experiments 3, 7, and 11 in Table 1) to 0.25–0.30 km^{-1} in the dusty atmosphere (experiments 1 and 2 in Table 1 were accompanied by intense transport of dust from the Sahara). For higher clouds (top altitude within 2–3 km), the ozone absorption band is clearly seen in spectral dependences of ω_0 and k (see Fig. 3*b*, curves *4* and *6*), whereas for lower clouds (top altitude less than 1 km) this absorption band is not observed.

If a fraction caused by molecular absorption is subtracted from the absorption coefficient, then the aerosol absorption shows no spectral dependence except for one case (Fig. 3*b*, curve *7*), in which the increase of k is observed as the wavelength increases. In this case, we can assume that the cloud contains organic fuel burning products according to Ref. 26, in which spectral absorption of these products was studied. Experiments 3 and 4 were conducted over the Black Sea and the Sea of Azov. Strong absorption bands are seen in curve *4*, Fig. 3*b*. These bands can be assigned to iron oxides Fe_nO_m according to the results of Refs. 27 and 28. Similar, but less pronounced, absorption bands are seen in the curves corresponding to the experiments 1 and 2 in the same figure. They also can be indicative of the presence of iron oxides in sand-laden air masses due to transport of sand from the Sahara.

Weak absorption bands near 0.4, 0.5, and 0.8 μm are likely caused by NaCl, as follows from Ref. 27. These bands are seen in the curve corresponding to the experiment 3, and they can be explained by the presence of sea salt in the atmospheric aerosol. It should be noted that absorption bands of atmospheric gases are more pronounced in the case of weak aerosol absorption and less pronounced when the aerosol absorption is stronger. The spectral values of co-albedo $(1 - \omega_0)$ for the experiments 6, 7, and 8 conducted in the same region are shown in Fig. 2*c*. In spite of the fact that the used measurements were made in different years, the results of reconstruction turned to be very close, and the values of $(1 - \omega_0)$ differ little in different experiments.

Effect of multiple scattering in a cloud

It should be emphasized that the values of ω_0 even for weakly absorbing clouds (type 1) are much less than the values obtained in model calculations by the Mie theory for an elementary cloud volume. The spectral dependence of the optical thickness (or the volume scattering coefficient) also does not find

explanation within the framework of the Mie theory. Propose a possible mechanism explaining the spectral dependence of the scattering coefficient of the cloud layer and high values of the absorption coefficient. This mechanism is connected with multiple scattering of radiation in a cloud, and it was already partially considered in Refs. 3 and 19.

In calculations of the radiation field in a cloud and description of the process of multiple scattering, the cloud layer is considered as additively superimposed on the molecular atmosphere. However, it is well known that, because of multiple scattering in an optically thick cloud, the mean number of collisions of a photon passing through an optically thick layer at pure scattering is proportional to τ^2 (Refs. 29 and 30) (for reflected photons the mean number of scattering events is proportional to τ). The photon path in a cloud elongates strongly as compared to the cloudless atmosphere, therefore the number of collisions with air molecules and particles of the atmospheric aerosol increases. Consequently, the contribution of molecular and aerosol scattering and absorption increases too. On the other hand, absorption withdraws some photons from this process and partially attenuates the effect of the growing role of molecular scattering.

The increase of the molecular and aerosol scattering and absorption due to elongation of the photon path in a cloud because of multiple scattering is considered in Refs. 3 and 19. Elongation of the photon path in a cloud was also considered in Refs. 31–34 when studying distortions of the shape of gas absorption bands in a cloud and in Ref. 35 when analyzing processes of scattering and absorption in the UV spectral region. The theory of multiple scattering and the equation of radiative transfer account for all processes of scattering and absorption, but only in the case that they are correctly taken into account in the model of the medium scattering and absorbing radiation.

Commonly, the equation of radiative transfer uses the mean values of initial parameters for the elementary volume of the scattering medium, and then the problem is solved by some or other method[29,30] of the theory of radiative transfer. It is important to choose the proper scale for the elementary volume, because it is different for each component of the medium. It should be also kept in mind that the parameters for the elementary volume of the medium should not be averaged at the initial stage of solving the physical problem. If atmospheric aerosols are located in a cloud outside droplets (such a case is called "external mixture"), then multiple scattering of radiation in a cloud intensifies the aerosol absorption. In Refs. 3 and 19, the empirical method was proposed, which can be used for transition from the values of the scattering and absorption coefficients α_{eff} and k_{eff} obtained from observations to the values α_{aer} and k_{aer} estimated using the theory of scattering.

In the case that aerosol particles are inside droplets ("internal mixture"), the aerosol absorption can be adequately taken into account in the equations for a single-component medium. In this connection, we can conclude that "anomalous" absorption is indicative of the external mixture of atmospheric aerosols and cloud droplets. In the cases considered above, the cloud medium is an external mixture, otherwise the absorption coefficient would coincide with the model values obtained from the theory of radiation scattering. The external mixture is likely produced in the case that atmospheric aerosol consists of hydrophobic particles (sand, soot, etc.). In contrast to hydrophilic particles, such atmospheric aerosols (consisting of sulfurous substances in many cases) increase absorption of the shortwave solar radiation in a cloud, not favoring the increase of the number of droplets in a cloud and its optical thickness.

The absorption coefficient k obtained from radiative experiments (see Table 2) can be transformed into the coefficient of aerosol absorption k_{aer} calculated using the theory of scattering with allowance made for multiple scattering by the equation[3,19]:

$$k_{\text{aer}} = k/(\tau^2 q) - k_{\text{mol}},$$

where τ is the optical thickness of a cloud; q is the coefficient depending on the true absorption and the geometric thickness of a cloud; k_{mol} is the coefficient of molecular absorption, which is nonzero in absorption bands of atmospheric gases.

This transformation gives the results shown in Table 3. For comparison, the table gives also the results of *in situ* measurements[39] and radiation absorption.[37,38,40] It follows from Table 3 that the absorption coefficient reconstructed from radiative measurements almost coincides with the data of direct measurements. Consequently, the role of atmospheric aerosols located outside cloud droplets and absorbing solar radiation was up to now underestimated when studying interaction of solar radiation and clouds because of neglect of the effect of multiple scattering of radiation by cloud droplets.

Table 3. Coefficients of absorption by atmospheric aerosols in cloud layer

Optical parameter	Type I – clear cloud	Type II – continental cloud	Type III – polluted cloud
k_{eff}, km^{-1}	< 0.02	0.08	0.25
τ^2	$16^2 = 256$	$9.5^2 = 90.25$	$8.7^2 = 75{,}69$
ω_0	0.9993	0.9970	0.9560
k_{aer}, km^{-1}, obtained from radiative measurements	$< 1 \cdot 10^{-4}$	$1.2 \cdot 10^{-3}$	$\sim 1 \cdot 10^{-1}$
k_{aer}, km^{-1}, direct measurements	$(1-10) \cdot 10^{-5}$ Ref. 39 $(1-12) \cdot 10^{-5}$ Ref. 38	$7 \cdot 10^{-4}$ Ref. 37	$(2.3-7.7) \cdot 10^{-2}$ Ref. 40

The allowance made for the effect of multiple scattering on the increase of the scattering coefficient in the shortwave region as compared to the wavelength of 0.8 μm leads to the dependences only a little differing from the spectral dependence of the Rayleigh scattering. Thus, we can conclude that the mutual effect of the multiple and Rayleigh scattering causes a marked spectral dependence of the scattering coefficient in a cloud.

Vertical profiles of optical parameters

The in-cloud observations[7,8,12] were used for reconstruction of optical parameters (volume scattering α and absorption k coefficients or optical thickness τ and single-scattering albedo ω_0) at different levels in a cloud. The technique of reconstruction is described in detail in Refs. 23, 41, and 42. To determine the in-cloud optical parameters, we used the data of three airborne experiments. Only in the experiment 7 the measurements were conducted with the height interval of 100 m, therefore just these measurements were taken as basic ones for the optical model of the vertical structure of a cloud. The smoothed values of the optical thickness and single scattering albedo for inner layers of a cloud are shown in Figs. 5–7 and Table 4.

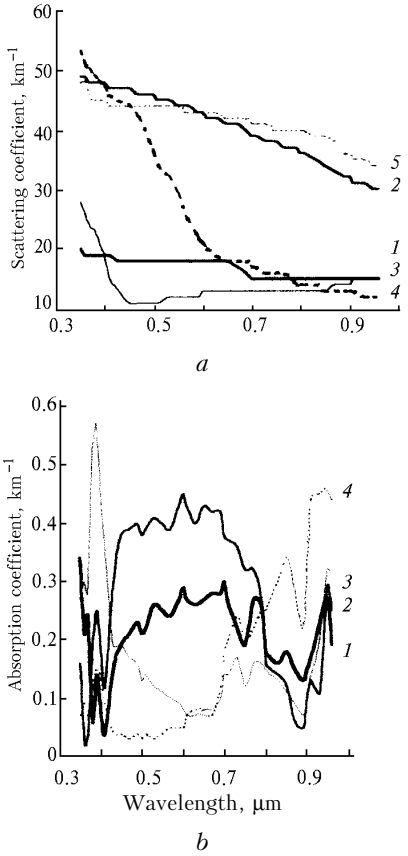

Fig. 5. Spectral dependence of volume scattering α (*a*) and absorption k (*b*) coefficients inside a cloud: layers of 1.4–1.3 (*1*), 1.3–1.2 (*2*), 1.2–1.1 (*3*), 1.1–0.9 (*4*), and 0.9–0.8 km (*5*).

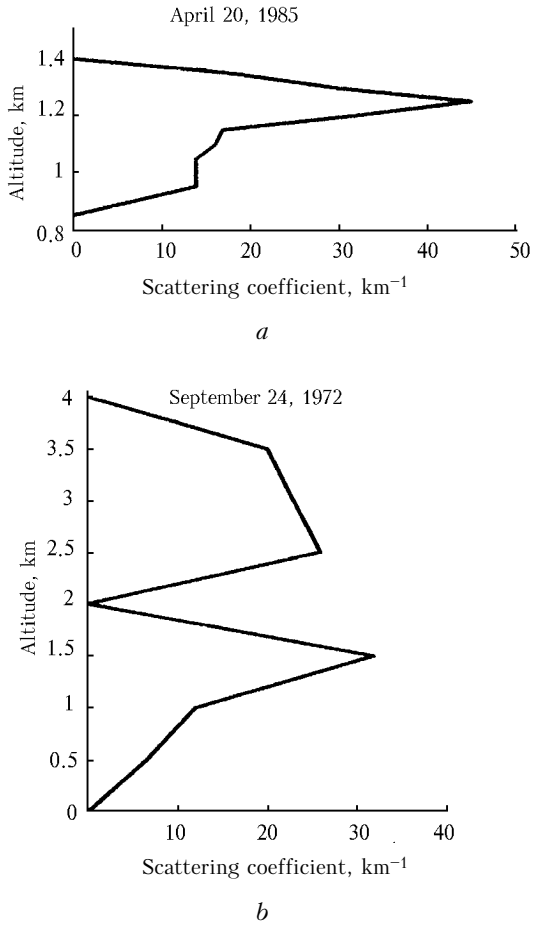

Fig. 6. Vertical profile of the scattering coefficient inside one-layer (*a*) and two-layer (*b*) stratus cloud.

The absorption coefficient k for the top cloud layer in the spectral region $\lambda > 0.8$ μm (< 0.02 km^{-1}) is smaller than for the middle and bottom layers. The Chappuis absorption band of ozone molecules appears only slightly in the upper layers and vanishes in the lower cloud layers. The absorption band nearby 0.40–0.41 μm is seen in all curves in Fig. 5*b*; according to Ref. 27, this band may be caused by the effect of nitrogen oxides.

The spectral behavior of the absorption coefficient in the bottom layer in the experiment 7 (curve *4* in Fig. 5*b*) coincides with the result obtained for the entire layer and, as was mentioned above, is characteristic of fuel burning products. It follows herefrom that the bottom part of a cloud accumulates absorbing atmospheric aerosols to a higher degree than the upper layers.

The vertical profiles of the optical parameters of a stratus cloud are shown in Figs. 6 and 7. The maximum scattering coefficient is in the central part of a cloud ($\alpha \sim 25$–40 km^{-1}) and the minimum near the cloud top and bottom. This result agrees well with the data obtained from airborne measurements over the Southern Ocean[43] and in the FIRE experiment.[44]

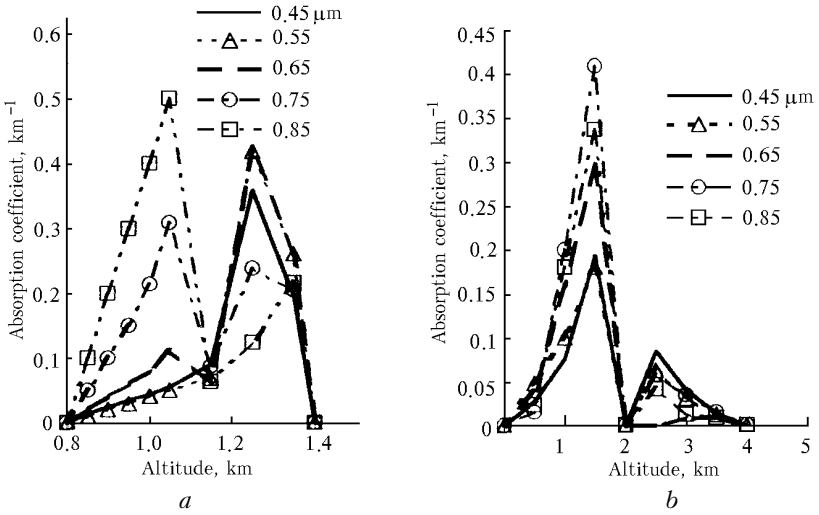

Fig. 7. Vertical profile of the absorption coefficient inside one-layer (*a*) and two-layer (*b*) stratus cloud.

Table 4. Single scattering albedo and optical thickness of different sublayers of stratus cloud

z*, km	1.4–1.3				1.3–1.2				1.2–1.1				1.1–0.95				0.95–0.8	
λ, μm	ω_0	k, km^{-1}	τ_1	α, km^{-1}	ω_0	k, km^{-1}	τ_2	α, km^{-1}	ω_0	k, km^{-1}	τ_3	α, km^{-1}	ω_0	k, km^{-1}	τ_4	α, km^{-1}	τ_5	α, km^{-1}
0.35	0.9831	0.34	2.0	20	0.9968	0.16	4.9	49	0.9949	0.27	5.3	53	0.9974	0.07	4.2	28	2.4	48
0.36	0.9891	0.21	1.9	19	0.9996	0.02	4.9	49	0.9942	0.30	5.1	51	0.9964	0.09	3.9	26	2.4	48
0.37	0.9876	0.24	1.9	19	0.9991	0.04	4.8	48	0.9944	0.28	5.0	50	0.9971	0.07	3.6	24	2.3	46
0.38	0.9971	0.06	1.9	19	0.9966	0.17	4.8	48	0.9899	0.50	4.9	49	0.9937	0.12	3.4	23	2.2	45
0.39	0.9925	0.14	1.9	19	0.9949	0.25	4.8	48	0.9881	0.57	4.8	48	0.9936	0.15	3.2	21	2.2	45
0.40	0.9961	0.07	1.9	19	0.9962	0.18	4.8	48	0.9906	0.45	4.7	47	0.9934	0.13	2.8	19	2.2	45
0.41	0.9977	0.04	1.9	19	0.9976	0.12	4.7	47	0.9920	0.37	4.6	46	0.9944	0.09	2.3	15	2.2	44
0.43	0.9920	0.15	1.8	18	0.9937	0.29	4.6	47	0.9957	0.19	4.5	45	0.9973	0.04	2.1	13	2.2	44
0.45	0.9889	0.19	1.8	18	0.9918	0.38	4.6	47	0.9956	0.19	4.4	44	0.9967	0.04	1.7	11	2.2	44
0.47	0.9876	0.21	1.8	18	0.9916	0.39	4.6	46	0.9960	0.17	4.2	42	0.9974	0.03	1.7	11	2.2	44
0.49	0.9867	0.23	1.8	18	0.9914	0.4	4.6	46	0.9959	0.16	3.8	38	0.9962	0.04	1.7	11	2.2	44
0.50	0.9876	0.21	1.8	18	0.9918	0.38	4.6	46	0.9964	0.13	3.6	36	0.9971	0.03	1.7	11	2.2	44
0.51	0.9873	0.22	1.8	18	0.9917	0.39	4.5	45	0.9960	0.14	3.4	34	0.9966	0.04	1.7	11	2.2	44
0.53	0.9859	0.26	1.8	18	0.9910	0.41	4.5	45	0.9963	0.12	3.2	32	0.9973	0.03	1.8	12	2.2	44
0.55	0.9857	0.25	1.8	18	0.9908	0.40	4.5	45	0.9961	0.11	2.7	29	0.9965	0.04	1.8	12	2.2	44
0.57	0.9858	0.24	1.8	18	0.9906	0.39	4.4	44	0.9961	0.10	2.6	25	0.9954	0.05	1.8	12	2.2	43
0.59	0.9854	0.27	1.8	18	0.9904	0.43	4.4	44	0.9960	0.09	2.2	22	0.9939	0.05	1.8	12	2.2	43
0.60	0.9842	0.29	1.8	18	0.9898	0.45	4.4	44	0.9960	0.08	1.9	21	0.9945	0.05	1.9	13	2.2	43
0.61	0.9850	0.27	1.8	18	0.9904	0.43	4.3	43	0.9961	0.07	1.9	20	0.9943	0.07	1.9	13	2.2	43
0.63	0.9858	0.26	1.8	18	0.9909	0.4	4.3	43	0.9962	0.07	1.9	19	0.9939	0.08	1.9	13	2.2	43
0.65	0.9852	0.27	1.8	18	0.9903	0.43	4.2	42	0.9956	0.08	1.8	18	0.9928	0.08	1.9	13	2.2	42
0.67	0.9839	0.28	1.7	17	0.9903	0.42	4.1	41	0.9950	0.08	1.8	18	0.9919	0.07	1.9	13	2.2	42
0.69	0.9825	0.28	1.6	16	0.9895	0.42	4.0	40	0.9944	0.10	1.8	18	0.9908	0.12	1.9	13	2.2	42
0.70	0.9804	0.3	1.5	15	0.9903	0.38	3.9	39	0.9920	0.14	1.7	17	0.9865	0.18	1.9	13	2.1	41
0.71	0.9829	0.26	1.5	15	0.9912	0.37	3.8	39	0.9920	0.14	1.7	17	0.9849	0.20	1.9	13	2.1	41
0.73	0.9866	0.22	1.5	15	0.9918	0.36	3.7	37	0.9913	0.17	1.6	16	0.9819	0.24	1.9	13	2.1	41
0.75	0.9874	0.19	1.5	15	0.9935	0.32	3.7	37	0.9933	0.12	1.6	16	0.9849	0.20	1.9	13	2.0	40
0.77	0.9822	0.27	1.5	15	0.9913	0.32	3.7	37	0.9895	0.16	1.6	16	0.9830	0.22	1.9	13	2.0	40
0.79	0.9870	0.26	1.5	15	0.9926	0.27	3.7	37	0.9884	0.16	1.4	14	0.9815	0.25	1.9	13	2.0	40
0.80	0.9879	0.18	1.5	15	0.9934	0.16	3.6	36	0.9898	0.14	1.4	14	0.9808	0.25	1.9	13	2.0	40
0.81	0.9889	0.17	1.5	15	0.9943	0.15	3.6	36	0.9899	0.14	1.4	14	0.9795	0.27	2.0	13	2.0	40
0.83	0.9897	0.16	1.5	15	0.9952	0.14	3.5	35	0.9903	0.13	1.4	14	0.9777	0.30	2.0	13	2.0	39
0.85	0.9871	0.18	1.5	15	0.9963	0.12	3.4	34	0.9944	0.11	1.3	13	0.9790	0.34	2.0	13	2.0	39
0.87	0.9902	0.15	1.5	15	0.9982	0.06	3.2	32	0.9927	0.09	1.3	13	0.9774	0.29	2.1	14	1.9	38
0.89	0.9894	0.13	1.5	15	0.9993	0.05	3.1	31	0.9923	0.07	1.3	13	0.9720	0.22	2.1	14	1.8	36
0.90	0.9875	0.15	1.5	15	0.9968	0.1	3.1	31	0.9890	0.10	1.3	13	0.9700	0.32	2.1	14	1.8	36
0.91	0.9899	0.17	1.5	15	0.9979	0.13	3.0	30	0.9836	0.14	1.3	13	0.9715	0.44	2.2	15	1.7	35
0.93	0.9874	0.23	1.5	15	0.9962	0.11	3.0	30	0.9838	0.20	1.2	12	0.9710	0.45	2.2	15	1.7	35
0.95	0.9826	0.27	1.5	15	0.9903	0.29	3.0	30	0.9737	0.32	1.2	12	0.9703	0.46	2.2	15	1.7	34
0.96	0.9873	0.19	1.5	15	0.9917	0.25	3.0	30	0.9744	0.31	1.2	12	0.9717	0.44	2.2	15	1.7	34

* Altitude of levels, at which the measurements were conducted.

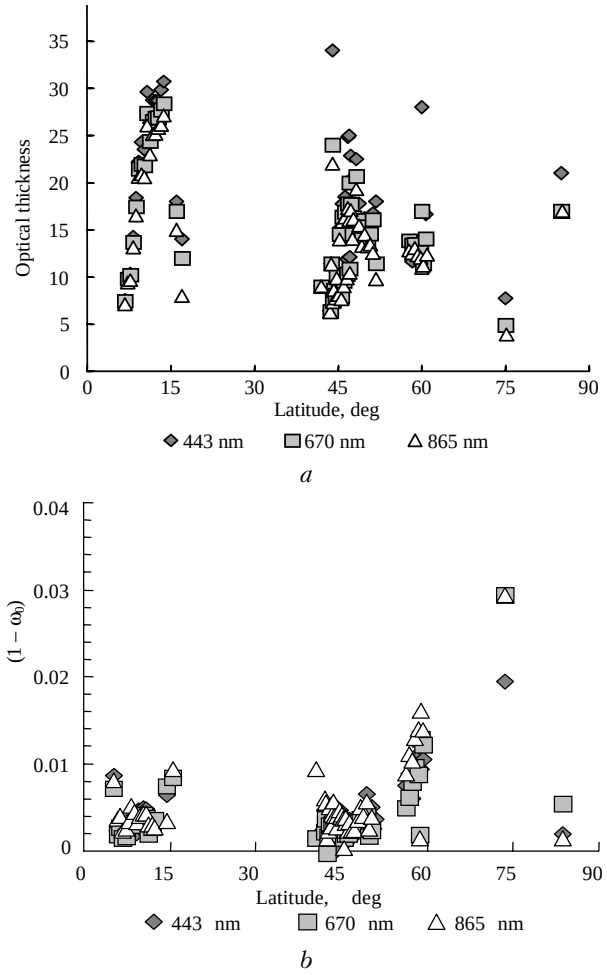

Fig. 8. Latitude distribution of the optical thickness (*a*) and single scattering co-albedo $(1 - \omega_0)$ (*b*) of stratus.

Spatial distribution of optical and radiative characteristics of stratus

As was mentioned above, the optical thickness and the single scattering albedo were determined from the data of space remote measurements[13,14] by the technique described in Refs. 22 and 25. Two NOAA-12 and NOAA-14 AVHRR images were considered along with seven ADEOS-I POLDER images. Since these images cover extended geographic regions, tentative analysis of the dependence of the optical parameters on the geographic location of clouds was performed. The obtained optical parameters, i.e., optical thickness and the single scattering albedo were averaged over latitude and longitude. The results presented in Figs. 8 and 9 do not show a marked difference in the values of the optical parameters for different geographic regions. Note that these results should be thought tentative, because we plan to process satellite data on the global scale for long time periods, as well as to conduct a thorough statistical analysis of the obtained results. Thereafter we will be able to judge reliably the peculiarities of geographic distribution and time variations of optical parameters of stratus clouds.

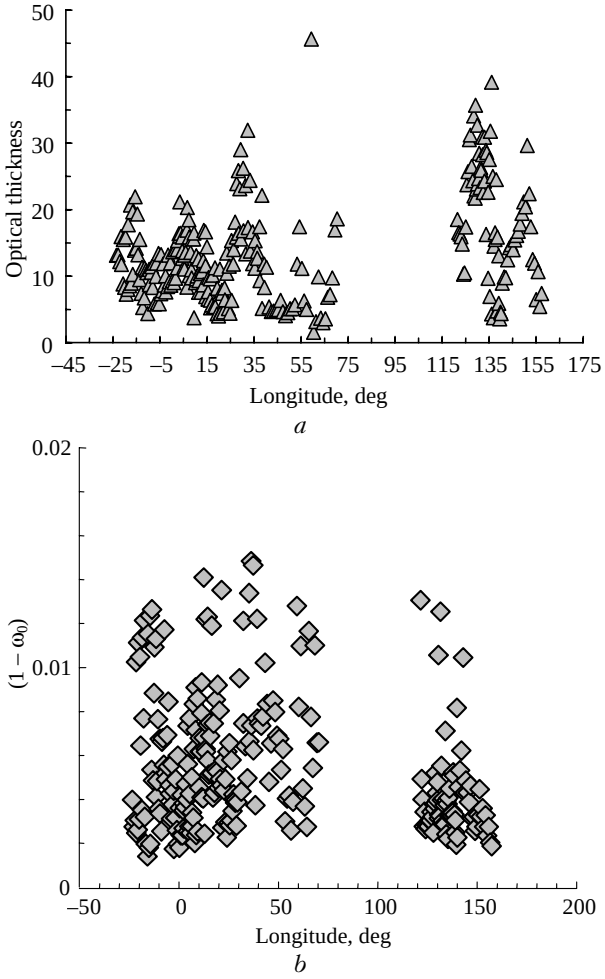

Fig. 9. Longitude distribution of the optical thickness (*a*) and single scattering co-albedo $(1 - \omega_0)$ (*b*) of stratus.

The optical parameters of clouds are interesting for analysis of the effect of clouds on the energy balance of the atmosphere. Therefore, the obtained averaged values of the optical thickness and single scattering albedo were used for calculation of radiative characteristics of the cloudy atmosphere: reflected and transmitted fluxes and absorbed solar radiation. Zenith angle of the sun in the calculations corresponded to local noon. Figure 10*a* shows the radiative characteristics (in relative units) of the flux, incident on the atmospheric top at the wavelength of 640 nm, as functions of geographic longitude. The obtained results show that the radiative characteristics are longitude-independent. Note the high value of the absorbed radiation ~ 10–20%, which points to the necessity to carefully take into account the effect of stratus clouds on warming of the atmosphere when constructing various scenarios of climate. It should be noted that these values of the absorbed radiation are obtained from airborne radiative measurements.[5–9] The characteristics of reflected, transmitted, and absorbed

radiation in the units of power W/m^2 are shown in Fig. 10*b* for the shortwave spectral region 400–900 nm in the cloudy atmosphere.

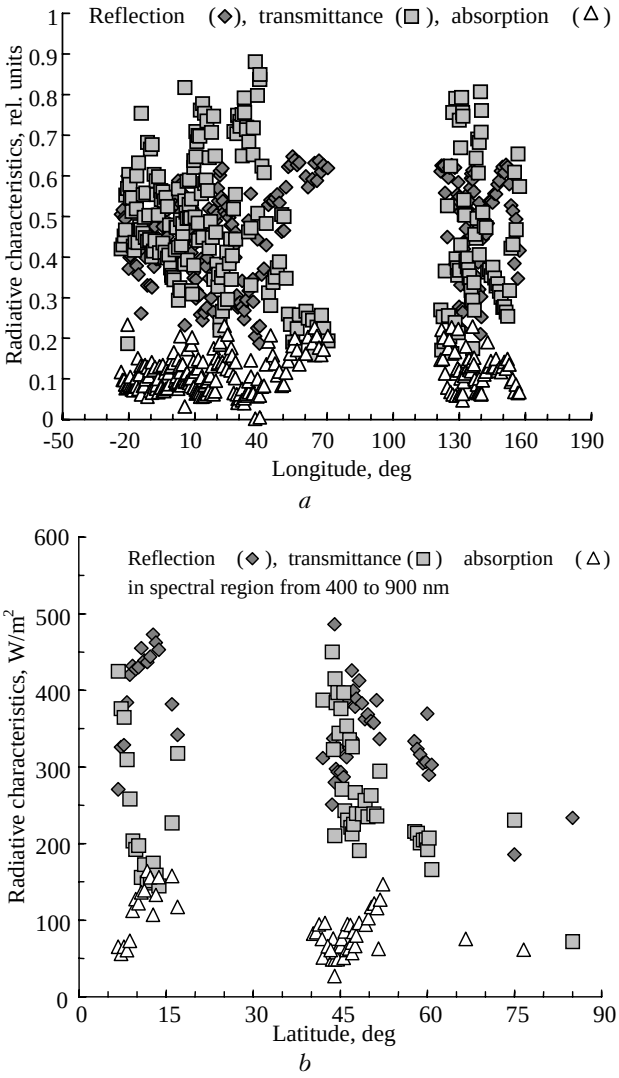

Fig. 10. Spatial distribution of radiative characteristics of stratus: reflected and transmitted fluxes and absorbed solar radiation in relative units of the flux incident on the atmospheric top as functions of longitude (*a*); reflected and transmitted fluxes and absorbed solar radiation in power units in the shortwave spectral region 400 - 900 nm as functions of latitude (*b*).

Conclusion

The results considered are the averaged data obtained from airborne and ground-based measurements in different regions and in different seasons. The spectral dependence of the scattering and absorption coefficients, optical thickness, and the single scattering albedo is presented. It was found that the role of absorbing atmospheric aerosols in radiative processes in a cloud increases because of interaction between atmospheric aerosols located outside cloud droplets and multiple scattering of radiation. Three types of stratus were distinguished according to the degree of radiation absorption: (1) weak true absorption (or conservative scattering at some wavelengths) $(1 - \omega_0) < 0.005$ observed over water or snow surfaces, (2) intermediate case $(1 - \omega_0) \sim 0.005–0.01$ observed over land, and (3) strong true absorption of radiation $(1 - \omega_0) \sim 0.01–0.05$ observed as a result of atmospheric transport of industrial pollutants or dust.

Gas absorption bands in the shortwave spectral region have different shapes in different clouds depending on the optical thickness of a cloud and the degree of radiation absorption by aerosols. The optical thickness and the volume scattering coefficient decrease markedly with the increasing wavelength. These facts can be explained by the effect of multiple scattering in a cloud.

The optical thickness of a one-layer cloud ranges from 10 to 20 at the wavelength $\lambda > 0.8$ μm. In high latitudes, clouds are weakly absorbing, and their optical thickness $\tau \le 10$ is less than in tropic latitudes.

The vertical profile of the optical parameters demonstrates maximum scattering coefficients at the center of a cloud layer and maximum absorption coefficients in its bottom part. It should be noted that more representative series of measurements are needed to make more reliable conclusions on vertical profiles of optical parameters of stratus. The spectral dependence of the absorption coefficients in different parts of a cloud layer points to different composition of atmospheric aerosols at different altitudes. Spectral dependence of the scattering coefficient in a cloud is observed only at sufficiently high values of the optical thickness.

The obtained results can be used in simulation of optical properties of stratus at radiative calculations in the shortwave spectral region.

References

1. H. Liao and J.H. Seinfield, J. Geophys. Res. D **103**, No. 4, 3781–3788 (1998).
2. J.M. Haywood and V. Ramaswamy, J. Geophys. Res. D **103**, No. 6, 6043–6058 (1998).
3. K.Ya. Kondratyev, V.I. Binenko, and I.N. Melnikova, Meteorol. Atmos. Phys. **65**, 1–10 (1998).
4. K.Ya. Kondratyev, V.I. Binenko, and I.N. Melnikova, Dokl. Ros. Akad. Nauk **345**, No. 6, 816–818 (1995).
5. K.Ya. Kondratyev, *Complex Atmospheric Energetic Experiment*, WMO GARP Publ. No. 12 (1972), 48 pp.
6. K.Ya. Kondratyev, V.I. Binenko, O.B. Vasilyev, and V.S. Grishechkin, in: *Proc. Int. Symp. Rad. Garmisch – Partenkirchen* (Science Press, 1977), pp. 572–577.
7. K.Ya. Kondratyev and V.I. Binenko, *Effect of Clouds on Radiation and Climate* (Gidrometeoizdat, Leningrad, 1984), 240 pp.
8. V.S. Grishechkin and I.N. Melnikova, in: *Rational Use of Natural Resources* (LPI, 1989), pp. 60–67.
9. V.S. Grishechkin, E.O. Shul'ts, and I.N. Melnikova, in: *Problems of Atmospheric Physics* (Leningrad State University Publishing House, Leningrad, 1989), Issue 20, pp. 32–42.

10. V.F. Radionov, G.G. Sakunov, and V.S. Grishechkin, in: *First Global Experiment PIGAP.* Part 2. *Polar Aerosol, Extended Cloudiness, and Radiation* (Gidrometeoizdat, Leningrad, 1981), pp. 89–91.
11. I.N. Melnikova, P.I. Domnin, C. Varotsos, and S.S. Pivovarov, Proc. SPIE **3237**, 77–80 (1997).
12. A.V. Vasil'ev, V.V. Mikhailov, and I.N. Melnikova, Izv. Ros. Akad. Nauk, Ser. Fiz. Atmos. Okeana **30**, No. 5, 630–635 (1994).
13. I.N. Melnikova, I. Galindo, and R. Solano, Atmos. Oceanic Opt. **12**, No. 3, 273–277 (1999).
14. I.N. Melnikova and T. Nakajima, Issled. Zemli iz Kosmosa, No. 3, 1–16 (2000).
15. V.V. Mikhailov and V.P. Voitov, in: *Problems of Atmospheric Physics* (Leningrad State University Publishing House, Leningrad, 1969), Issue 6, pp. 175–181.
16. V.V. Gorodetskii, M.N. Maleshin, S.Ya. Petrov, E.A. Sokolova, V.I. Pchelkin, and S.P. Solov'ev, Opt. Zh. **62**, No. 7, 3–9 (1995).
17. I.N. Melnikova and V.V. Mikhailov, J. Atmos. Sci. **51**, 925–931 (1994).
18. I.N. Melnikova, Atm. Opt. **4**, No. 1, 39–45 (1991).
19. I.N. Melnikova, Atmos. Oceanic Opt. **5**, No. 2, 116–120 (1992).
20. I.N. Melnikova and V.V. Mikhailov, Dokl. Ros. Akad. Nauk **328**, No. 3, 319–321 (1993).
21. I.N. Melnikova and P.I. Domnin, Atmos. Oceanic Opt. **10**, No. 6, 455–459 (1997).
22. I.N. Melnikova, P.I. Domnin, and V.F. Radionov, Izv. Ros. Akad. Nauk, Ser. Fiz. Atmos. Okeana **34**, No. 6, 669–676 (1998).
23. I.N. Melnikova, Atmos. Oceanic Opt. **11**, No. 1, 1–6 (1998).
24. S. Asano, WCRP-86 (WMO/TD No. 648) (WMO, Geneva, 1994), pp. 72–73.
25. I.N. Melnikova, P.I. Domnin, V.V. Mikhailov, and V.F. Radionov, J. Atmos. Sci. **57**, No. 6, 623–630 (2000).
26. I.N. Sokolik, Izv. Akad. Nauk SSSR, Ser. Fiz. Atmos. Okeana **24**, No. 3, 345–357 (1988).
27. L.S. Ivlev and S.D. Andreev, *Optical Properties of Atmospheric Aerosols* (Leningrad State University Publishing House, Leningrad, 1986), 360 pp.
28. I. Sokolic and O.B. Toon, J. Geophys. Res. D **104**, No. 8, 9423–9444 (1999).
29. E.G. Yanovitskii, *Light Scattering in Inhomogeneous Atmospheres* (Kiev, 1995), 400 pp.
30. I.N. Minin, Astrofiz. Akad. Nauk Arm. SSR **17**, No. 3, 585–618 (1981).
31. B.G. Dianov-Klokov, E.I. Grechko, and G.P. Malkov, Izv. Akad. Nauk SSSR, Ser. Fiz. Atmos. Okeana **9**, No. 5, 524–537 (1973).
32. K. Pfeilsticker, F. Erle, O. Funk, L. Marquard, T. Wagner, and U. Platt, J. Geophys. Res. D **103**, No. 19, 35323–35335 (1998).
33. T. Wagner, F. Erle, L. Marquard, C. Otten, K. Pfeilsticker, T. Senne, J. Stutz, and U. Platt, J. Geophys. Res. D **103**, No. 19, 25307–25321 (1998).
34. K. Pfeilsticker, J. Geophys. Res. D **104**, No. 43, 4101–4116 (1999).
35. B. Mayer, A. Kylling, S. Madronich, and G. Seckmeyer, J. Geophys. Res. D **103**, No. 23, 31241–31254 (1998).
36. K.Ya. Kondratyev, ed., *Aerosol and Climate* (Gidrometeoizdat, Leningrad, 1991), 542 pp.
37. A.D. Clarke, Appl. Opt. **21**, 3011–3020 (1982).
38. A.D. Clarke, Aerosol Sci. Technol. **10**, 161–171 (1989).
39. C.H. Twohy, A.D. Clarke, S.G. Warren, L.F. Radke, and R.J. Charlson, J. Geophys. Res. D **94**, No. 6, 8623–8631 (1989).
40. R.E. Waggoner, A.P. Weiss, N.C. Ahlquist, D.S. Covert, and R.J. Charlson, Atmos. Environ. **15**, 1891–1909 (1981).
41. K.Ya. Kondratyev, V.I. Binenko, and I.N. Melnikova, Atmos. Oceanic. Opt. **11**, No. 4, 331–337 (1998).
42. Melnikova and V. Mikhailov, J. Geophys. Res. D **105**, No. 18, 23255–23273 (2000).
43. R. Boers, J.B. Jensen, P.B. Krummel, and H. Gerber, Quart. J. Roy. Meteorol. Soc. **122**, 1307–1339 (1996).
44. J.A. Curry, P.V. Hobbs, M.D. King, D.A. Randall, P. Minnis, G.A. Isaac, J.O. Pinto, T. Uttal, A. Bucholtz, D.G. Cripe, H. Gerber, C.W. Fairall, T.J. Garrett, J. Hudson, J.M. Intrieri, C. Jakob, T. Jensen, P. Lawson, D. Marcotte, L. Nguyen, P. Pilewskie, A. Rangno, D.C. Rogers, K.B. Strawbridge, F.P.J. Valero, A.G. Willams, and D. Wylie, Bulletin of the American Meteorological Society **81**, No. 1, 5–29 (2000).